Mechanisms of Electrochemically-Induced Retro-Cyclopropanation Reactions of Fullerene Derivatives Using Digital Simulations

Maurizio Carano[b] and Luis Echegoyen*[a]

Abstract: Three C_{60} derivatives, **1**, **2** and **3**, have been studied by cyclic voltammetry (CV) under high vacuum in anhydrous tetrahydrofuran (THF). The CV behavior was essentially similar to that already observed for other cyclopropanated fullerene derivatives. After the second reduction processes all compounds undergo a chemical reaction that generates another electroactive species. This "new" chemical species is likely to be the compound with the cyclopropane ring open. Differences in CV behavior were observed for the different addends. Electrochemical data obtained at different scan rates for a given potential window, were fit with the BAS digital simulation program, DigiSim. The purpose of this study was to probe the proposed mechanisms and to obtain reliable estimations of the kinetic constants for the homogeneous chemical reactions taking place during the CV experiments. Calculations at the PM3 level lend additional support to the conclusions derived from digital simulations. The proposed mechanism is similar for all the compounds and involves two main chemical reactions in a reversible square scheme.

Keywords: cyclic voltammetry · digital simulation · electrochemistry · fullerenes · retro-cyclopropanation

Introduction

The discovery of the retro-Bingel reaction[1] was made by electrolyzing a CH_2Cl_2 solution of diethyl 1,2-methano-[60]-fullerene-61,61-dicarboxylate (in 0.1 M Bu_4NPF_6) at 293 K at a controlled potential of -1.55 V (vs Ag). The applied potential corresponded to that for the voltammetric formation of the dianion, but during the 30 min of the bulk electrolysis experiment, four electrons per molecule were transferred. Analysis of the products after reoxidation of the solution at 0 V followed by column chromatography yielded pure C_{60} in over 80% yield. Equivalent experiments conducted with C_{60}, C_{70}, and C_{76} derivatives led to the use of this reaction as a synthetic tool in fullerene chemistry.[2a] Additional work resulted in the discovery of an intramolecular electrochemically-induced isomerization of C_{60} bis-adducts.[2b] Exhaustive reduction (at -1.2 V vs Ag) with one electron per molecule resulted in seven regioisomers regardless of which pure bis-adduct regioisomer was electrolyzed. These bis-adducts were successively separated and chemically and electrochemically characterized.

Some spiromethanofullerenes were also found to be unstable after multiple reduction processes,[3] and CPE experiments have led to the isolation of C_{60} in high yields. Thus the electrochemical removal of methano-adducts is not limited to the malonate derivatives of fullerenes (Bingel adducts). A more recent study was conducted in THF to avoid the well-known reactivity of CH_2Cl_2 towards the polyanions of C_{60}[4] and to explore the mechanisms involved during adduct removal.[5] Surprisingly, an electrochemically induced intermolecular adduct transfer was observed for the spiromethanofullerenes studied, but not for the diethyl 1,2-methano-[60]-fullerene-61,61-dicarboxylate. The regioisomer distribution found in THF differed significantly from that obtained when the compounds are prepared by a direct synthetic route.[1, 5] The proposed mechanism for the formation of bis-adducts during the CPE timescale involves the presence of two distinct pathways. When the reductive electrochemistry leads to the cleavage of one of the two cyclopropane bridging bonds, the intermediate is capable of either losing the addend from the fullerene cage or of reacting with another fullerene molecule. This could lead to the formation of dimers in which the two fullerene cages share one or two addends.

Because of its generality and ease, the retro-cyclopropanation reaction has been used as a synthetic tool for various purposes.[1–7] The "Bingel – retro-Bingel" strategy as a protection – deprotection scheme has already found several appli-

[a] Prof. L. Echegoyen
Clemson University, Department of Chemistry
219 Hunter Chemistry Laboratories
P.O. Box 340973, Clemson, SC 29634-0973 (USA)
Fax: (864)-656-6613
E-mail: luis@clemson.edu

[b] Dr. M. Carano
Department of Chemistry and Biochemistry
University of Texas, Austin, TX 78712 (USA)

DOI: 10.1002/chem.200204407

cations in fullerene derivative synthesis and in higher fullerene isomer chemistry[8] and electrochemistry.[7] Taking advantage of the fact that covalent adducts of isomeric higher fullerenes are much easier to separate than the parent unfunctionalized carbon spheroids, it was possible to isolate two major isomers and a third minor isomer of C_{84} in pure form. When different addends are present on the same C_{60} sphere, it is also possible to selectively remove the bis(alkoxycarbonyl)methano addend. The Bingel addend can therefore play the role of a protecting group and also direct unusual multiple addition patterns.[8]

As mentioned above, the mechanism of these retro-cyclopropanation reactions is still not understood although some work has been done in our group and in others to gain better knowledge of the processes involved. Nuretdniov et al.[9] reported a study based on the electrochemical characterization of four C_{60} derivatives. Based on the number of exchanged electrons, and using Nicholson's treatment,[10] they reported rate constants for chemical processes involved in the retro-cyclopropanation reaction. However, the proposed mechanism was not supported by simulations or product characterizations. Additionally, there are internal inconsistencies, since C_{60} is supposed to be formed, yet no anodic peaks assignable to C_{60} are observed.

Here we report an electrochemical study of three C_{60} derivatives (Scheme 1) by cyclic voltammetry, and a mechanistic study using digital simulations.[11–15] Theoretical calculations using PM3 further support the hypothesis formulated in this work.

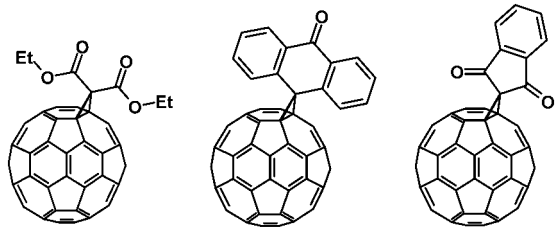

1 2 3

Scheme 1. Structures of the compounds studied.

Results and Discussion

Compounds **1**–**3** were studied using cyclic voltammetry in THF under aprotic conditions.[16] This solvent was the most suitable for a cathodic investigation and provided good solubility for the compounds selected.[17] For a given potential window, several scans at different rates were performed. This provided a wide range of experimental conditions for appropriate data fitting of the proposed mechanism. The best fitting is obtained by the optimization of the kinetic parameters for the electrochemically induced homogeneous chemical reactions. The three compounds were chosen because they all give retro-cyclopropanation reactions after the second electron reduction of the C_{60} cage, but at the same time, each of them exhibits a distinct and characteristic CV behavior. The electrochemistry of **1** is mainly characterized by the appearance of a small peak after the second reduction process. This peak is not assignable to C_{60} and the addend is not electroactive at this potential. The following reduction is irreversible, and when the scan is reversed after this latter process the new peak is more evident than in the forward scan. Compound **2** has been reported[18] and the reduction potentials and orbital energies are available. Its behavior is somewhat similar to that of **1**. Compound **3** has a 1,3-indandione addend and exhibits a different CV pattern when compared to **1** and **2** under the same experimental conditions.

Electrochemical investigations of C_{60} derivatives: All CV scans were limited to the first three reduction processes in order to focus our attention on the first stages of the electrochemically induced decomposition of these compounds. These derivatives can be reduced by more than three electrons within the experimentally available potential window, leading to further, and even more complicated, ECC and/or ECEC mechanisms. Interestingly, and somehow surprisingly, it was clear that the first two C_{60} centered reduction processes are reversible for all three compounds. This means that even if chemical reactions are taking place, the processes are reversible on the CV timescale and the starting compound is recovered at the end of the experiment.

Figure 1a shows the CV for a 0.5 mM THF solution of **1** (using a Pt disk as working electrode). We can observe three main reduction processes, the first two being reversible and the third one chemically irreversible. The small peak between the second and third C_{60}-based reductions is designated II*. This peak, which is barely discernible under these experimental conditions, becomes more evident if the scan rate is decreased. We can better appreciate the presence of this redox process if, at lower scan rates, we reverse the CV scan right after the potential at which it occurs (Figure 1b). This peak is always observed while performing cyclic voltammetry for this compound, as has been reported by many different research groups, and the ratio between its height and that of the other peaks is always the same under identical experimental conditions (scan rate and temperature in this case).

As mentioned above, the cathodic peak II^*_c completely disappears upon increasing the scan rate from 0.2 to 1 $V s^{-1}$ (Figure 1c solid line); this indicates that this process is due to some unstable species, perhaps an intermediate, arising from a chemical reaction. On the contrary, its anodic counterpart II^*_a increases in height also with respect to the other peaks when the sweep is faster (Figure 1c solid bold line).

A second reaction pathway following the reduction process at peak III leads to the same intermediate chemical species in a higher reduction state. It was assumed that the reoxidation of the product of the latter homogeneous chemical reaction takes place at II^*_a. Since peak III is still irreversible when the scan rate is increased and the current function for peak II_a is lower than at lower scan rates, it can be argued that the rate constant for the backward chemical reaction is not high enough to regenerate the original concentration of the starting compound.

Increasing the scan rate up to 10 $V s^{-1}$ did not improve chemical reversibility for peak III. Limiting the scan to peak

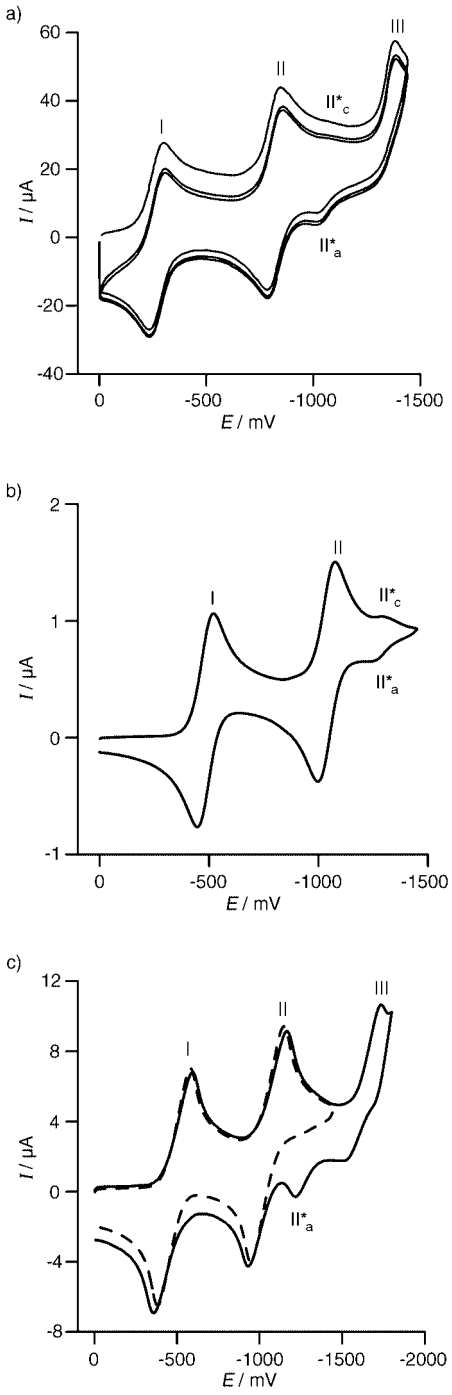

Figure 1. a) Cyclic voltammogram for a 0.5 mM THF solution of **1** at $v = 0.5\ V s^{-1}$, Pt as working electrode, Pt-mesh counter electrode and Ag wire as a quasi-reference electrode, $T = 25\,^{\circ}C$. Multiple cycles have been performed without the renewal of the diffusion layer. b) $v = 0.05\ V s^{-1}$, concentration of **1** is 0.1 mM; c) $v = 1\ V s^{-1}$, concentration of **1** is 0.1 mM.

II* only, it was possible to observe how it disappeared at scan rates higher than $1\ V s^{-1}$ (Figure 1c dotted line).

These experimental results are fully in agreement with those previously obtained in our group using other solvents.[3] From the analysis of these results, it is possible to have an idea of the difference between the rate constants for the homogenous reactions occurring after peaks II and III.

The CV for an analogous solution of compound **2** is shown in Figure 2. It is clear that the pattern is very different from that observed for compound **1** and, while peak I remains reversible, peak II is chemically irreversible. The third reduction process is almost fully reversible, indicating that if a

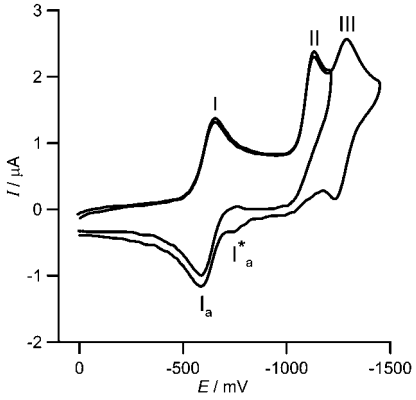

Figure 2. Cyclic voltammetric curves for a 0.5 mM THF solution of **2** at $v = 0.5\ V s^{-1}$, Pt as working electrode, Pt-mesh counter electrode and a Ag wire as a quasi-reference electrode, $T = 25\,^{\circ}C$.

chemical reaction is coupled with the electron transfer it is not fast enough on the experimental timescale. Interestingly, a new peak (I_a*) appears as a shoulder on peak I_a in the reverse scan at potentials slightly more cathodic (approximately 80 mV) with respect to $E_{1/2}$ for peak I. Nevertheless peak I appears to be fully reversible under all experimental conditions. Even if the scan is reversed after peak II (and for $v = 0.2\ V s^{-1}$), peak I remains irreversible but peak I_a* is no longer present, suggesting that the chemical reaction occurs only after the third reduction process. A similar effect was observed by performing the complete scan, including peak III, at a scan rate of at least $3\ V s^{-1}$.

It is known that the antraquinone unit gives an irreversible first reduction process,[18] which can be confidently assigned to peak II. Thus it seems that for compound **2** the retrocyclopropanation reaction takes place after the third reduction of the molecule and at this stage, this is apparently not a fast process on the experimental CV timescale.

The most complicated CV behavior was found for compound **3**, which undergoes an initial two electron reduction followed by another process which is 700 mV more cathodic (Figure 3, continuous line). Interestingly, an intermediate irreversible peak was found (II) whose intensity increases with the scan rate relative to the other two peaks. At $v = 3\ V s^{-1}$, the current function ratios between peaks I, II and III are evidently different (Figure 3, dotted line) from those at $0.2\ V s^{-1}$ (Figure 3, solid line). Even if the scan is stopped after peak II, there is no improved reversibility of this second process. Increasing the scan rate increases the distance between cathodic and anodic peaks for I but not for III (while the irreversible reduction at II is shifted towards more negative potentials). This means that the observed effect on the rate of the electron transfer is not exclusively the result of the ohmic drop since it affects only one portion of the CV. This feature and the general shape of the curve is reminiscent

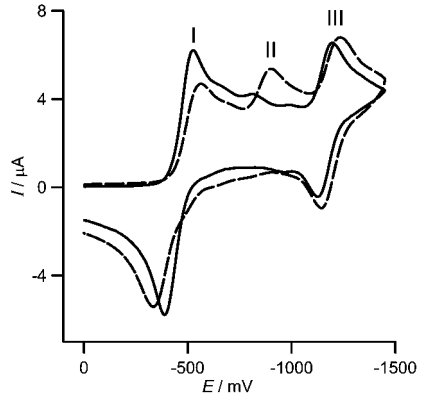

Figure 3. Cyclic voltammetric curves for a 0.5 mM THF solution of **3** at $v = 0.5\ V s^{-1}$ (——) and $3\ V s^{-1}$ (- - - -), Pt as working electrode, Pt-mesh counter electrode and a Ag wire as a quasi-reference electrode, $T = 25\,^{\circ}C$. The current for the scan at $3\ V s^{-1}$ is divided by a suitable factor, i.e., the ratio between the square roots of the scan rates ($3^{1/2}/0.5^{1/2}$). This treatment allows a direct comparison of the height of the peaks at different scan rates.

of a bi-electronic slow electron transfer process.[19] By convolutive analysis[20] it was possible to calculate the number of electrons for peaks I, II and III. This number was found to be equal to approximately 1.9, 0.1 and 0.9, respectively, at $0.2\ V s^{-1}$ and to 1.6, 0.4 and 0.9 at $3\ V s^{-1}$. This is in agreement with the fact that peak II is due to the reduction of an intermediate and that it is possible to observe this species if the scan rate is increased. After this further reduction, peak III remains always reversible and its height behaves as predicted by theory.[13]

Digital simulations: The effects of mass transport, electron transfer kinetics and the kinetics of the coupled chemical reactions (if there are any) on a cyclic voltammogram cannot be easily separated. The extraction of quantitative information, such as rate constants for the preceding or following chemical reactions from such a series of experimental results typically requires comparison of the latter with simulated data or with predictions derived from a theoretical model.[21, 22] When considering chemical reactions coupled to electron transfer it has to be taken into account that any variation from reversible behavior is related not to the absolute magnitude of the rate constant for the chemical reaction, but to the value of this rate constant relative to the timescale of the experiment.[23] Thus increasing the scan rate of the experiment (i.e., decreasing its timescale), also decreases the time available for the chemical reaction to take place and hence the effect of the latter can be decreased or even eliminated.[24] It is important to realize that for a given CV, there might be several mechanisms and parameter value sets that provide a good match between the experimental and simulated data. Therefore it is necessary to acquire a wide set of the experimental CVs, run under different conditions (scan rate and concentration of reagents, for instance), in order to provide good support for the fitting. This approach greatly increases the chances to find reliable values for those parameters governing the mechanism for the studied process, and minimizes the risk of finding a relative minimum during the fitting procedure. Some of the parameters used were measured (such as $E_{1/2}$ and E_{peak} potentials) and some were assigned based on previously published values (electron transfer rates and diffusion coefficients).[25] The remaining parameters for the homogeneous chemical reactions were fitted to the experimental curves.

Digital simulation experiments are a powerful tool for confirming reaction mechanisms and for evaluation of the relevant kinetic[26] and thermodynamic ($E_{1/2}$,[27] K_{eq}[28]) parameters. One of the commercially available software packages for digital simulation of cyclic voltammetries is DigiSim, which is currently used widely to support experimental observations.[29]

The kinetic parameters reported in this article provided the best fits between experiment and theory for cyclic voltammetry experiments. In order to check if true minima had been found, the fitting routine was also run using different starting values for the selected parameters.

Compound 1: Based on the available experimental evidence the reaction mechanism proposed and tested by digital simulation is that shown on the right of Figure 4a. In this scheme there are three reduction processes in which the starting compound (A) is involved and two homogeneous chemical reactions that lead to a new species (B). The new species is also electroactive and this electrochemical process, the reduction of B leading to B1, closes a square Scheme that also involves the di- and tri-anions of A. This Scheme accounts for the main features of the recorded CVs. A slow initial chemical reaction accounts for the smooth peak (II^*_c) observed in the forward scan (Figure 4a, left side) and another, fast reaction accounts for the irreversibility of the third reduction. Peaks I and II are reversible for all the scan rates recorded. This is in agreement with a reversible chemical reaction like the above-mentioned opening of the cyclopropane ring. Values of the kinetic constants are reported in Table 1.

Table 1. Kinetic parameters obtained from the simulations for compounds **1**–**3**. Electron transfer processes were considered fast ($k = 10^4\ s^{-1}$) and electron transfer coefficients (α) were assumed to be equal to 0.5.

	k^{I}_{f}	k^{I}_{b}	k^{II}_{f}	k^{II}_{b}
1	$6 \times 10^{-3}\ s^{-1}$	$9 \times 10^{-2}\ s^{-1}$	$6 \times 10^{2}\ s^{-1}$	$3 \times 10^{-2}\ s^{-1}$
2	$\approx 0\ s^{-1}$	$10^{5}\ s^{-1}$	$0.7\ s^{-1}$	$0.2\ s^{-1}$
3	$2\ s^{-1}$	$4\ s^{-1}$	$7 \times 10^{2}\ s^{-1}$	$4 \times 10^{-6}\ s^{-1}$

On the CV timescale, it is not likely that C_{60} will form in appreciable amounts. Performing multiple scans without the renewal of the diffusion layer shows that the original compound is reformed after every cycle, confirming this prediction. However, a mechanism involving C_{60} as a product on the voltammetric timescale has been proposed.[9] This hypothesis was tested via digital simulation. The rate constant for the first chemical reaction reported in that article was used in the Scheme in Figure 4a. The simulation is in agreement with the experimental curve for the forward scan but not with that for the backward. Another simulation was performed assuming that C_{60} is formed as reported in the same article.

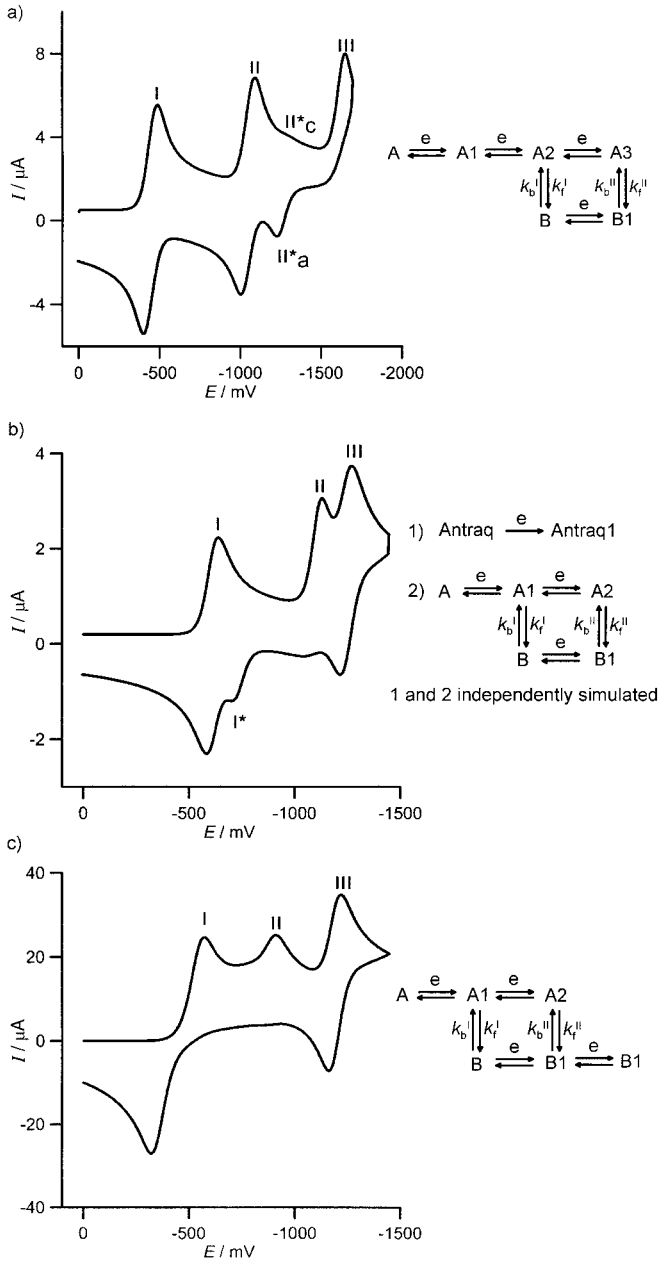

Figure 4. a)–c) are the best simulated curves (on the left side) for compounds **1**–**3**, respectively, following the mechanisms shown on the right side of the figure. a) and b) at 0.5 Vs^{-1}, c) at 3 Vs^{-1}.

Thus the known C_{60} reduction potentials were assigned to the new species in the simulated mechanism (B in the present case). The values for E_p reported in the article were also used in the simulation, which showed a reversible third reduction while the first reoxidation peak was split into two. This simulation was not in agreement with the experimental results reported in that article or with those reported in here. A final simulation was performed using the mechanism proposed by the authors together with the kinetic parameters reported in the table. This led to a multi-electronic peak for the third wave and to split oxidation processes for II and I. Once again, these results are far from the experimentally recorded voltammograms. Since the redox potentials for the starting compound and those for C_{60} are substantially different, it would be evident from the position of the reoxidation peaks if C_{60} was the main product of the retro cyclopropanation reaction on the CV timescale.[9] In fact, even if some C_{60} was formed during the sweep, it must be a very small quantity because it is not detected in the experimental voltammograms.

In order to further test this hypothesis, Figure 5 shows the simulated voltammogram for the same mechanism of Figure 4a, but considering that the product of the homogeneous

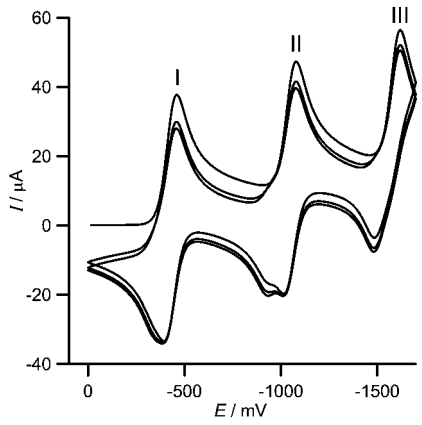

Figure 5. Digital simulation based on mechanism shown in Figure 1a and assuming that the final product (B) of the homogeneous reaction is C_{60}. Redox potentials for C_{60} in the same experimental conditions are available in literature.[35]

reaction B is C_{60}. Therefore the known redox potentials for this molecule were assigned to the new chemical species. It is evident how the CV is substantially different from the experimental one (Figure 1a). In particular, peak III is now more reversible but at the same time its anodic component is shifted towards less negative potential. Also the shape of peak I is different from the experimental one while two reoxidation processes are clearly present in the potential region of peak II. The simulation of multiple scans shows how these features are even more evident after the first cycle.

As already reported, digital simulations were performed over a wide range of scan rates and concentration values to fit the experimental curves. As found experimentally, while changes in concentration did not affect the morphology of the voltammograms, changes in sweep rates had a considerable impact on the curves. As an example, Figure 6 shows an experimental and a simulated curve (continuous and dotted line, respectively), for **3**. The first one was acquired under the same experimental conditions as in Figure 3 at 0.5 Vs^{-1}, and the simulation was performed following the Scheme and using the parameters of Figure 4c. The only parameter changed with respect to Figure 4 was the scan rate. Even if the two curves don't overlap perfectly (partly due to a higher background current in the experimental curve after the first reduction peak), the agreement between the simulated and the experimental curves is very good. In particular, the height of peak II decreases for both curves (Figure 3 dotted line and Figure 4) as predicted by the mechanism.

Compound 2: The CV behavior for compound **2** (Figure 2) is evidently different from that of compound **1** because the

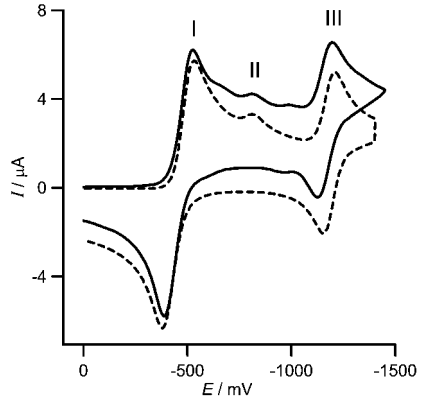

Figure 6. Cyclic voltammetric curves for a 0.5 mM THF solution of **3** at $\nu = 0.5\ V s^{-1}$ (——) and simulated curve based on mechanism shown in Figure 4c (- - - -) for the same scan rate. Pt as working electrode, Pt-mesh counter electrode and an Ag wire as a quasi-reference electrode, $T = 25\,^{\circ}C$.

anthrone addend is capable of undergoing a reduction process within the scanned potential window.[18] Since this process is electrochemically irreversible and its redox potential is -1.59 V vs Fc^{+}/Fc, it is likely that this unit is responsible for the appearance of peak II. At this potential one electron is mainly localized on the fullerene cage and another one on the addend and these are non-interacting units. This is a reasonable assumption since the difference between the reduction potential of anthrone and its corresponding redox potential in compound **2** is quite small. Peak III probably corresponds to the second reduction of the fullerene group and it is reasonably reversible. Only a very small portion of the reduction current is not fully recovered in the anodic part of the process. This is probably due to a chemical reaction of the tri-reduced species. The final simulation mechanism used for this compound (Figure 4b, right side) turned out to be essentially the same as the one found for compound **1** (i.e., a square mechanism). In this case the chemical instability of this C_{60} derivative shows up after the third reduction process (reaction 2), that is, after a two electron reduction of the fullerene unit and a one electron reduction of the anthrone addend. This chemical reaction leads to the formation of an electroactive species which is reoxidized in I* (mechanism ECE with a square scheme). After this reoxidation process, a fast chemical reaction (reaction 1, see Table 1 for the value of the kinetic constant) reforms the starting compound in its mono reduced state (A1). This chemical step accounts for the chemical reversibility of peak I. The irreversible reduction process of the addend is not included in the main Scheme since its redox state does not seem to affect the chemical behavior of the starting compound.[30–32] The second and third reduction potentials for compound **2** were essentially identical to those measured for the first reduction of anthrone and the second reduction for a substituted C_{60},[33–35] respectively, indicative of very weak electronic interactions between the addend and the fullerene core. The calculated kinetic constant for the chemical reaction occurring after the third reduction wave was found to be quite small ($0.7\ s^{-1}$) and is reported, with other data, in Table 1. This explains why peak III is almost reversible and peak I* disappears if the scan rate is increased. As can be seen from the simulated mechanism and from the calculated kinetic constant values, the first chemical equilibrium is totally displaced towards the mono-reduced starting compound. The agreement between the experimental curves and those obtained with the digital simulation program was good for all of the scan rates recorded.

Compound 3: In contrast to the other compounds, the electroactivity of the addend in compound **3** greatly influences the overall electrochemical behavior. The simulation shown in Figure 4c was made using the mechanism shown on the right side of the figure. This path takes into account both the new experiments and previously published data.[5] The most challenging feature of the pattern to simulate was the increasing height of the second reduction peak with an increase of the scan rate. As previously explained, if the rate of the potential sweep is increased, the height of this peak increases while that of peak I decreases (peak I is bielectronic at $0.02\ V s^{-1}$ and becomes closer and closer to monoelectronic as the scan rate is increased). Peak II is totally irreversible within the scan rate range investigated ($0.02\ V s^{-1}$, $20\ V s^{-1}$). After many attempts it was possible to simulate this interesting pattern by assuming that after the first reduction (peak I, first electron) a subsequent reaction forms a new species (B) which has the same reduction potential (or perhaps even less negative) than that of the starting molecule (peak I second electron). The fraction of the monoanion of the original species (A) that does not undergo the chemical reaction is then responsible for peak II. This is an irreversible process because at this stage another homogenous reaction transforms A2 into B1. Since increasing the scan rate increases the height of peak II, it is clear that the first chemical reaction (A1 leading to B) is not extremely fast on the experimental timescale (see values in Table 1). After peak II, the remaining starting compound is transformed into the new one (B1) and after this stage this new chemical species is capable of accepting reversibly another electron. Comparison of the rate constants obtained from the simulation shows that both processes are not very fast for these sweep rates, even if the forward kinetic constant for the second reaction is in the range of $10^{3}\ s^{-1}$. Nevertheless the second reduction is irreversible with a rate constant for the backward process of $10^{-6}\ s^{-1}$. If the scan rate is increased, part of the anodic component of I shifts towards less negative potential because the chemical equilibrium is displaced (square scheme on the right side of Figure 4c). Therefore, there is not enough time for A1 to be regenerated after the reoxidation of B1 to B during the reverse scan. This shift is due to the relatively low value of k^{1}_{b}. In the simulations, as well as in the experimental results, the anodic peak (that always corresponds to a two-electron wave) is broader than the cathodic one due to this chemical conversion. Nevertheless, as A1 is formed it is readily reoxidized to A since the redox potential for this couple is more negative than that for B and B1.

Semiempirical calculations: Two extreme structures were optimized for all the compounds, one with the cyclopropane ring intact and another with the ring open. PM3 calculations were performed to determine orbital energies of the neutral and the mono reduced species. A study, at the PM3 level, of

the electronic structure of some spiroannelated methanofullerenes has been previously reported by Wudl and co-workers.[33] Since results for compound **2** were reported in that article, it was possible to validate our work by reproducing those data. The LUMO for **1** was found to be at −2.80 eV. Adding electrons and calculating the energies for both open and closed structures showed that the open geometry becomes slightly favored after the second electron addition. This explains the slow rate constant found for the first chemical reaction that, according to the mechanism, leads to the cleavage of the cyclopropane ring. The cathodic shift found experimentally for **2** with respect to C_{60} is smaller than the one reported for the same compound in the literature. A possible explanation, which agrees with the results reported in the same article, is the different experimental conditions (solvent and supporting electrolyte). The first reduction occurs at a potential 88 mV more cathodic than the first reduction of C_{60}.[34, 35] The value for the calculated energy of the LUMO in the neutral species was in perfect agreement with that reported in the literature (−2.84 eV).[33] The LUMO energy for the mono-reduced compound was found to be −2.75 eV for the closed structure, while that found for the open structure was too high in energy to represent a reasonable alternative. The electron density for this orbital confirms that the second reduction involves mainly the anthrone unit. At this point it is important to recall that, according to the electrochemical data, the second electron transferred to **2** is located on the quinone-type ligand. According to the published result, the two units (namely the C_{60} cage and the anthrone addend) are electrochemically independent. This means that the second reduction has no effect on the stability of the cyclopropane ring. Thus after the second reduction there is no cleavage of the cyclopropane ring since electrons are localized one on each group. Only when the third electron is transferred, that is when the second electron reduction occurs on the C_{60} cage, cleavage of the cyclopropane occurs. This process is quite slow ($k_f = 0.7\ s^{-1}$ according to the mechanism) indicating that the conversion of the starting compound into a new chemical species is far from complete on the CV timescale. The closed structure of **3** has a −2.88 eV value for the LUMO energy. This is in agreement with the first reduction process which occurs at a slightly more cathodic potential relative to that of C_{60}, where the LUMO is located at −2.89 eV. As previously reported,[33a] the first electron is based on C_{60} and the spin density was found to be different for the closed and the open structures. In fact, while for the closed structure the unpaired electron density is mainly localized on the C_{60} moiety, the open cyclopropane structure has the unpaired electron density residing mainly on the addend. The closed structure shows a LUMO for the mono-anion that is too high in energy to explain the experimental CV behavior in which the first two electrons are transferred at the same potential. On the other hand, the open structure of $\mathbf{3}^{\bullet-}$ has a new orbital localized on the 1,3-indandione addend (due to the structural rearrangement of the molecule after the opening of the cyclopropane ring), and its energy is between the HOMO and the LUMO of the C_{60} cage. The orbital is half occupied by the electron corresponding to the first reduction process. The second electron is therefore expected to be localized in the addend, and this explains the two electron reduction process found for this compound. The open structure of $\mathbf{3}^{\bullet-}$ is stabilized by about 19 kcal mol^{-1} according to PM3 calculations. This provides a good explanation for the coincidence of the two reduction waves.

Conclusions

For the first time a systematic study to determine the kinetic parameters for the electrochemically induced retro-cyclopropanation reaction was carried out using digital simulations. The study was conducted with three different C_{60} derivatives in which the addends result in different electrochemical responses. They range from the non-electroactive addend in **1** to the electroactive and highly interacting unit in compound **3**, while in **2** the antraquinone moiety is an electroactive species that interacts poorly with the fullerene cage. This wide range of characteristics explains the differences between the proposed mechanisms for the compounds. On the other hand, many common features were found, such as the necessity for the description of these processes to include a square Scheme mechanism in order to regenerate the starting compound, on the CV timescale. Comparing the rate constants at the same reduction stage of the C_{60} core, that is, when the same number of electrons has been transferred to the fullerene cage shows that the rate for the cleavage of the cyclopropane ring increases in going from **1** to **3**. Compound **1** is the simpler case studied since all of its redox processes are exclusively C_{60} centered. Digital simulations confirmed the proposed mechanism and allowed the estimation of the rate constants of the chemical reactions.

Compound **2** was found to be unstable only after the third reduction process because the two components of the molecule have weak electronic coupling. The reduction of the addend does not seem to affect the structure of the molecule. Experimental CVs, digital simulations (i.e., calculated kinetic constants) and calculations demonstrate that cyclopropane ring opening is slow. It is actually possible to minimize its effect by simply increasing the scan rate by about an order of magnitude (from 0.5 to 3 V s^{-1}).

In contrast to **1** and **2**, **3** is unstable after the first reduction process. The mechanism involves cleavage of the cyclopropane ring after the first electron reduction. At slower scan rates, a second electron is transferred at the same potential as the first one. Increasing the scan rate allows the observation of the increase of the height of the intermediate peak (II) which is due to the original species.

Experimental Section

C_{60} derivatives (10^{-3} M) and supporting electrolyte Bu_4NPF_6 (10^{-1} M) were added into a home built electrochemical cell. The cell was degassed and pumped to 10^{-6} mm Hg. The solvent, THF (previously dried using a Na/2K amalgam and stored under argon), which had also been degassed and pumped to the same pressure, was then vapor-transferred into the cell, directly from the storing flask. All CVs were recorded in THF (NBu_4PF_6 as supporting electrolyte) using a Pt disc (1 mm diameter) as a working

electrode, a Pt-mesh counter electrode and a Ag wire as a quasi-reference electrode. The potential of the Ag wire was assumed to be stable within the CV timescale. Ferrocene was added, under an argon flux, at the end of the measurements as an internal standard. For digital simulations the BAS program, DigiSim version 3.03 (CV), was used. The Wavefunction software, PC-Spartan pro was used at the PM3 level for the semiempirical calculations.

Acknowledgements

The authors wish to thank the Chemistry Division of the National Science Foundation, grant CHE 0135786, for generous support of this work.

[1] R. Kessinger, J. Crassous, A. Hermann, M. Rüttimann, L. Echegoyen, F. Diederich, *Angew. Chem.* **1998**, *110*, 2022–2025; *Angew. Chem. Int. Ed.* **1998**, *37*, 1919–1922.
[2] a) R. Kessinger, M. Gómez-López, C. Boudon, J.-P. Gisselbrecht, M. Gross, L. Echegoyen, F. Diederich, *J. Am. Chem. Soc.* **1998**, *120*, 8545–8546; b) L. E. Echegoyen, F. D. Djojo, A. Hirsch, L. Echegoyen, *J. Org. Chem*. **2000**, *65*, 4994–5000.
[3] M. W. J. Beulen, L. Echegoyen, J. A. Rivera, M. Á. Herranz, Á. Martín-Domenech, N. Martín, *Chem. Commun.* **2000**, 917–918.
[4] M. W. J. Beulen, L. Echegoyen, *Chem. Commun.* **2000**, 1065–1066.
[5] a) M. W. J. Beulen, J. A. Rivera, M. Á. Herranz, Á. Martin-Domenech, N. Martin, L. Echegoyen, *Chem. Commun.* **2001**, *5*, 407–408; b) M. W. J. Beulen, J. A. Rivera, M. Á. Herranz, B. Illescas, N. Martín, L. Echegoyen, *J. Org. Chem*. **2001**, *66*, 4393–4398.
[6] G. A. Burley, P. A. Keller, S. G. Pyne, G. E. Ball, *Chem. Commun.* **2001**, *6*, 563–564.
[7] a) J. Crassous, J. Rivera, N. S. Fender, L. Shu, L. Echegoyen, C. Thilgen, A. Hermann, F. Diederich, *Angew. Chem.* **1999**, *111*, 1716–1721; *Angew. Chem. Int. Ed.* **1999**, *38*, 1613–1617; b) R. Kessinger, N. S. Fender, L. E. Echegoyen, C. Thilgen, L. Echegoyen, F. Diederich, *Chem. Eur. J.* **2000**, *6*, 2184–2192.
[8] a) W. Qian, Y. Rubin, *Angew. Chem*. **1999**, *111*, 2504–2508; *Angew. Chem. Int. Ed.* **1999**, *38*, 2356–2360; b) F. Cardullo, L. Isaacs, F. Diederich, J.-P. Gisselbrecht, C. Boudon, M. Gross, *Chem. Commun*. **1996**, 797–799; c) F. Cardullo, P. Seiler, L. Isaac, J.-F. Nierengarten, R. F. Haldimann, F. Diederich, T. Mordasini-Denti, W. Thiel, C. Boudon, J.-P. Gisselbrecht, M. Gross, *Helv. Chim. Acta* **1997**, *80*, 343–371.
[9] I. A. Nuretdinov, V. V. Yanilkin, V. P. Gubskaya, N. I. Maksimuyuk, L. Sh. Berezhnaya, *Russ. Chem. Bull.* **2000**, *49*, 427–430.
[10] R. S. Nicholson, J. Shain, *Anal. Chem.* **1965**, *37*, 190–195.
[11] a) D. Britz, *Digital Simulation in Electrochemistry*, Springer, Berlin, **1988**; b) S. W. Feldberg, *Digital Simulation in Electroanalytical Chemistry*, *Vol. 3* (Ed. A. J. Bard), Marcel Dekker, New York, **1969**.
[12] A. J. Bard, L. R. Faulkner, *Electrochemical Methods*, 2nd ed., Wiley, **2000**.
[13] I. Rubinstein, *Physical Electrochemistry*, Marcel Dekker, **1995**.
[14] a) S. A. Lerke, D. H. Evans, S. W. Feldberg, *J. Electroanal. Chem.* **1990**, *296*, 299–315; b) A. C. Michael, R. M. Wightman, C. A. Amatore, *J. Electroanal. Chem*. **1989**, *267*, 33–45.
[15] a) C. Amatore, G. Farsang, E. Maisonhaute, P. Simon, *J. Electroanal. Chem.* **1999** *462*, 55–62; S. Kim, S. Yun, C. Kang, *J. Electroanal. Chem*. **1999**, *465*, 153–159; b) F. Paolucci, M. Marcaccio, C. Paradisi, S. Roffia, C. A. Bignozzi, C. Amatore, *J. Phys. Chem. B* **1998**, *102*, 4759–4769; c) T. Nann, J. Heinze, *Electrochem. Commun.* **1999**, *1*, 289–294.
[16] J. Heinze, *Angew. Chem.* **1984**, *96*, 823–840; *Angew. Chem. Int. Ed. Engl*. **1984**, *23*, 831–847.
[17] M. Carano, P. Ceroni, L. Mottier, F. Paolucci, S. Roffia, *J. Electrochem. Soc.* **1999**, *146*, 3357–3360.
[18] T. Ohno, N. Martín, B. Knight, F. Wudl, T. Suzuki, H. Yu, *J. Org. Chem.* **1996**, *61*, 1306–1309.
[19] B. Tulythan, W. E. Geiger, *J. Am. Chem. Soc.* **1985**, *107*, 5960–5967.
[20] L. Nadjo, J. M. Saveant, *J. Electroanal. Chem.* **1973**, *48*, 113–145.
[21] K. Y. Lee, C. A. Amatore, J. K. Kochi, *J. Phys. Chem*. **1991**, *95*, 1285–1294.
[22] D. Kosynkin, T. M. Bockman, J. K. Kochi, *J. Am. Chem. Soc*. **1997**, *119*, 4846–4855.
[23] J. O'M. Bockris, A. K. N. Reddy, *Modern Electrochemistry*, *Vol. I*, Plenum, New York, **1998**.
[24] a) C. Amatore, S. Szunerits, L. Thouin, J. S. Warkocz, *Electrochem. Commun*. **2000**, *2*, 353–358; b) C. Amatore, F. Bonhomme, J. L. Bruneel, L. Servant, L. Thouin, *Electrochem. Commun.* **2000**, *2*, 235–239; c) C. Amatore, S. Szunerits, L. Thouin, *Electrochem. Commun*. **2000**, *2*, 248–253; d) C. Amatore, B. Fosset, J. Bartlet, M. R. Deakin, R. M. Wightman, *J. Electroanal. Chem*. **1988**, *256*, 255–268; e) C. P. Andrieux, P. Hapiot, J. M. Saveant, *J. Electroanal. Chem.* **1993**, *349*, 299–309; f) C. P. Andrieux, A. Anne, J. Moiroux, J. M. Saveant, *J. Electroanal. Chem*. **1991**, *307*, 17–28; g) D. Garreau D, J. M. Saveant, *J. Electroanal. Chem*. **1978**, *86*, 63–73.
[25] a) W. R. Fawcett, M. Opallo, M. Fedurco, J. W. Lee, *J. Am. Chem. Soc*. **1993**, *115*, 196–200; b) W. R. Fawcett, M. Opallo, M. Fedurco, J. W. Lee, *J. Electroanal. Chem*. **1993**, *344*, 375–381; c) D. Dubois, M. T. Jones, K. M. Kadish, *J. Am. Chem. Soc.* **1992**, *114*, 6446–6451; d) D. Dubois, G. Moninot, W. Kutner, M. T. Jones, K. M. Kadish, *J. Phys. Chem*. **1992**, *96*, 7137–7145; e) P. M. Allemand, A. Koch, F. Wudl, Y. Rubin, F. Diederich, M. M. Alvarez, S. J. Anz, R. L. Whetten, *J. Am. Chem. Soc.* **1991**, *113*, 1050–1051; f) D. Dubois, K. M. Kadish, S. Flanagan, R. E. Haufler, L. P. F. Chibante, L. J. Wilson, *J. Am. Chem. Soc.* **1991**, *113*, 4364–4366; g) D. Dubois, K. M. Kadish, S. Flanagan, L. J. Wilson, *J. Am. Chem. Soc.* **1991**, *113*, 7773–7774.
[26] M. F. Gueves da Silva, J. A. L. da Silva, J. J. R. Frausto da Silva, A. J. Pombeiro, C. Amatore, J. N. Verpeaux, *J. Am. Chem. Soc.* **1996**, *118*, 7568–7573.
[27] M. Marcaccio, F. Paolucci, C. Paradisi, S. Roffia, C. Fontanesi, L. J. Yellowlees, S. Serroni, S. Campagna, C. Denti, V. Balzani, *J. Am. Chem. Soc.* **1999**, *121*, 10081–10091.
[28] a) M. R. Bryce, G. Cooke, F. M. A. Duclairoir, V. M. Rotello, *Tetrahedon Lett*. **2001**, *42*, 1143–1145; b) A. Niemz, A. Cuello, L. K. Steffen, B. F. Plummer, V. M. Rotello, *J. Am. Chem. Soc*. **2000**, *122*, 4798–4802; c) A. Niemz, V. M. Rotello, *J. Am. Chem. Soc*. **1997**, *119*, 6833–6836; d) R. Deans, G. Cooke, V. M. Rotello, *J. Org. Chem*. **1997**, *62*, 836–839.
[29] a) B. A. Brookes, P. C. White, N. S. Lawrence, R. G. Compton, *J. Phys. Chem. B* **2001**, *105*, 6361–6366; b) L. J. Nunez-Vergara, M. Bonta, J. C. Sturm, P. A. Navarrette, S. Bollo, J. A. Squella, *J. Electroanal. Chem*. **2001**, *506*, 48–60; c) R. Antiochia, I. Lavagnini, F. Magno, *Electroanalysis* **2001**, *13*, 582–586; d) E. Potteau, E. Levillain, J. P. Lelieur, *J. Electroanal. Chem*. **1999**, *476*, 15–25; e) J. A. Alden, A. M. Bond, R. Colton, R. G. Compton, J. C. Eklund, Y. A. Mah, P. J. Mahon, V. Tedesco, *J. Electroanal. Chem*. **1998**, *447*, 155–171; f) J. A. Alden, F. Hutchinson, R. G. Compton, *J. Phys. Chem. B* **1997**, *101*, 949–958.
[30] a) A. A. Vlcek, *Coord. Chem. Rev.* **1982**, *43*, 39–62; b) A. A. Vlcek, *Revue De Chemie Minerale* **1983**, *20*, 612–627.
[31] A. Kaifer, M. G. Kaifer, *Supramolecular Electrochemistry*, Wiley-VCH, Weinheim, **1999**.
[32] A. Vlcek Jr., J. Heyrovsky in *Electron Transfer in Chemistry*, *Vol. 2*, Part 2 (Ed. V. Balzani), Chapter 5, Wiley-VCH, Weinheim, **2001**.
[33] a) B. Knight, N. Martin, T. Ohno, E. Orti, C. Rovira, J. Veciana, J. Vidal-Gancedo, P. Viruela, R. Viruela, F. Wudl, *J. Am. Chem. Soc*. **1997**, *119*, 9871–9882; b) M. Eiermann, R. C. Haddon, B. Knight, Q. C. Li, M. Maggini, N. Martin, T. Ohno, M. Prato, T. Suzuki, F. Wudl, *Angew. Chem.* **1995**, *107*, 1755–1758; *Angew. Chem. Int. Ed. Engl*. **1995**, *34*, 1591–1594.
[34] L. Echegoyen, L. E. Echegoyen, F. Diederich, in *Fullerenes*, K. M. Kadish, R. S. Ruoff, Wiley, New York, Chapter 11, **2000**.
[35] T. Da Ros, M. Prato, M. Carano, P. Ceroni, F. Paolucci, S. Roffia, *J. Am. Chem. Soc*. **1998**, *120*, 11645–11648.

Received: September 11, 2002 [F4407]

